Available online at www.sciencedirect.com

ScienceDirect

Scripta Materialia 97 (2015) 1–4

Scripta MATERIALIA

www.elsevier.com/locate/scriptamat

Solubility of zirconium and silicon in molybdenum studied by first-principles calculations

O. Lenchuk,* J. Rohrer and K. Albe

Institut für Materialwissenschaft, TU Darmstadt, Jovanka-Bontschits-Str. 2, D-64287 Darmstadt, Germany

Received 6 August 2014; revised 15 September 2014; accepted 7 October 2014
Available online 29 October 2014

We investigate the solubility of zirconium and silicon in molybdenum using a supercell approach within the framework of electronic density-functional theory. The heat of solution is calculated for various supercells and an extrapolation procedure is applied to correct for finite-size effects. An analysis of size (lattice distortion) and chemical (bond strength) contributions to the heat of solution is applied to explain different solubility limits of Zr and Si. The charge redistribution around substitutionals is quantitatively estimated using a Bader charge analysis.

Keywords: Bcc molybdenum; Solubility; First-principle calculation; Refractory metals

1. Introduction

Mo-based alloys combine high strength and stiffness at elevated temperatures with high thermal conductivity and a low coefficient of thermal expansion desired for high-temperature applications [1–3]. Because of their creep and corrosion resistance they bear good prospects to be used in turbine blades [4].

In order to meet the requirements for the desired applications, other material properties such as ductility and fracture toughness have to be comparable with traditionally used Ni-based superalloys. Experimental studies show that microalloying with Zr is an efficient way to increase the fracture toughness and ductility of both, binary Mo–Si [5] and ternary Mo–Si–B [6,4] alloys. Since the solubility limit for Zr in Mo is still a matter of debate, it is unclear if the experimentally observed results can be attributed to grain boundary or bulk effects. Ham [7], for instance, examined Mo arc-cast alloys and found a solubility of 3–5 at.% Zr at 1373 K. Okamoto [8], in contrast, has reported a value of 10 at.% Zr dissolved in bcc-Mo at 2153 K. Rudy [9] and Brewer [10], in contrast, reported a Zr solubility of 18–20 at.% at around 2223 ± 50 K.

While Zr is increasing the ductility, Si is known to significantly increase the strength due to solid solution strengthening and thus reduce the room-temperature ductility. Most importantly, Si is also improving the oxidation resistance of Mo–Si–B alloys due the formation of a protective borosilicate glass [11,12]. When the system is supersaturated with silicon, SiO_2 particles are formed at grain boundaries at elevated temperatures and passivate the system. Experimental high-temperature measurements report a solubility of ≈4 at.% Si in Mo [13–15]. However, a theoretical assessment of the heat of solution is still lacking and would provide helpful insights for the alloy design.

In this study, we present density-functional theory (DFT) calculations [16,17] of the heat of solution of Zr and Si in Mo and analyse size effects and chemical contributions. The systems are characterized electronically using a Bader change analysis and density of states (DOS). The results are also useful for understanding grain boundary segregation and diffusion mechanisms in polycrystalline molybdenum.

2. Method

Supercells constructed from a $(2 \times 2 \times 2)$ to a $(5 \times 5 \times 5)$ replication of the conventional Mo bcc cell with a single substitutional atom are considered. This results in a total of 16 up to 250 atoms and a solute concentration of 6.25 at.% to 0.4 at.%.

Total-energy calculations are performed using the projector-augmented planewave code vasp [18,19] in conjunction with the PBE [20] exchange-correlation functional. Careful convergence studies of the heat of solution are performed for each cell size. We use an energy cutoff of 450 eV and Monkhorst–Pack grid [21], where the number of **k**-points is chosen such that the heat of solution is converged to at least 5 meV. Structural optimization procedures are stopped after residual forces on individual atoms were smaller than 0.01 eV/Å^2. Atoms are relaxed under different boundary conditions: (a) constant pressure ($p = 0$) and (b) constant volume.

---

* Corresponding author; e-mail: lenchuk@mm.tu-darmstadt.de

http://dx.doi.org/10.1016/j.scriptamat.2014.10.007

Table 1. Comparison of calculated Mo properties to experiment and other abinitio calculations.

	a_0 (Å)	B_0 (GPa)
Present study	3.15	268
Experiments [24,25]	3.147	272–273
Other computational studies [26]	2.988	263–291

Based on the supercell calculations, the heat of solution of Zr is calculated as

$$H_{\mathrm{s,Zr}} = E_{\mathrm{Mo}_x\mathrm{Zr}_y} - y \cdot \epsilon_{\mathrm{Mo_2Zr}} - (x - 2y) \cdot \epsilon_{\mathrm{Mo}}. \tag{1a}$$

For Si, the heat of solution is obtained from

$$H_{\mathrm{s,Si}} = E_{\mathrm{Mo}_x\mathrm{Si}_y} - y \cdot \epsilon_{\mathrm{Mo_3Si}} - (x - 3y) \cdot \epsilon_{\mathrm{Mo}}. \tag{1b}$$

In Eq. (1a) and Eq. (1b) $E_{\mathrm{Mo}_x(\mathrm{Zr,Si})_y}$ is the total energy of the defective Mo supercell containing a solute atom. The total energy of bulk molybdenum per Mo atom is represented by ϵ_{Mo}. To minimize errors, both $E_{\mathrm{Mo}_x(\mathrm{Zr,Si})_y}$ and ϵ_{Mo} are calculated using the same set of **k**-points. Mo_2Zr is used as a reference state for Zr, since the pure Mo phase is in equilibrium with the Mo_2Zr phase if the Zr content is increased [8]. Similarly, for the calculations of Si the Mo_3Si phase [13] is taken in equilibrium with the Mo phase.

The relaxation volume is computed according to [22]

$$V_{\mathrm{rel}} = 1/3 \cdot Tr(P_{\alpha\beta}) V_0 / B_0. \tag{2}$$

Here $p = 1/3 \cdot Tr(P_{\alpha\beta})$ is the hydrostatic part of the stress tensor, that corresponds to the increase in pressure due to the presence of the defect in the material with the equilibrium volume V_0 and the bulk modulus B_0.

At a given temperature T the heat of solution can be used to compute the solid solubility limit using [23]

$$c = \exp(-H_{\mathrm{s}}/k_{\mathrm{B}}T), \tag{3}$$

where k_{B} is the Boltzmann constant.

3. Results and discussion

Table 1 lists the lattice constant (a_0) and bulk modulus (B_0) of Mo obtained in the present study. The bulk modulus is obtained by fitting the energy variation upon hydrostatically deforming the Mo cell to a Birch–Murnhagen equation of state [27]. Both a_0 and B_0 are in a good agreement with other experimental and theoretical studies [24–26].

Figure 1 shows the calculated heat of solution H_{s} of Zr and Si obtained according to Eq. (1a) and (1b) as a function of the reciprocal number of atoms ($1/N$) in the cell. For each solute atom, two data sets are shown along with linear extrapolations. The red data points correspond to H_{s} obtained from calculations at constant volume; the black data points correspond to calculations at zero pressure. Thus, independent of the computational settings, the extrapolation of the computed data points gives the same value, which represents the heat of solution of Zr (Si) in the dilute limit: the heat of solution for Zr is $H_{\mathrm{s,\ Zr}} = 0.27 \pm 0.03$ eV and for Si we receive $H_{\mathrm{s,\ Si}} = 0.87 \pm 0.03$ eV. The positive sign of the heat of solution indicates that the dissolution of Zr (Si) from Mo_2Zr (Mo_3Si) into Mo as a solid solution is an endothermic process. The relaxation volumes of Zr and Si are calculated according to Eq. (2) and represent the increase in pressure due to the presence of the solute in a host lattice. We find that V_{rel} is weakly depending on the cell size approaching a value of 0.16 Ω for Zr, where Ω is the atomic volume of Mo, and −0.10 Ω for Si. Positive and negative values of the relaxation volume correspond to an expansion or contraction of the cell, respectively.

Table 2 lists the calculated heat of solution and the equilibrium solubility, obtained at the temperature of peritectic reaction "$L + Mo_{\mathrm{bcc}} \rightarrow Mo_2Zr$" for Zr and "$L + Mo_{\mathrm{bcc}} \rightarrow Mo_3Si$" for Si, using Eq. 3 and the calculated values of the heat of solution (in a diluted regime).

The calculated solubilities are slightly higher than the experimental ones, which is most likely due to the neglection of formation entropies and the assumption of the dilute limit. However, the theoretical value for Zr confirms the experimental finding that Zr content of 20% are possible under equilibrium conditions.

For getting a better understanding, why Zr and Si solubility in Mo are considerably different, we subdivide the calculated heat of solution into mechanical and chemical contributions according to Finnis et al. [28]. The first term represents the energy stored mechanically due to the size misfit of the solute in the solvent lattice. The second describes the chemical solute–solvent interatomic interactions. Figure 2 shows a schematic picture of the individual contributions to the heat of solution. The size contribution consists of two steps labeled (b) ⟶ (a) "Host Removal (HR)" and (c) ⟶ (a) "Substitutional Structure (SuSt)" [28]. It corresponds to the energy required to remove a host

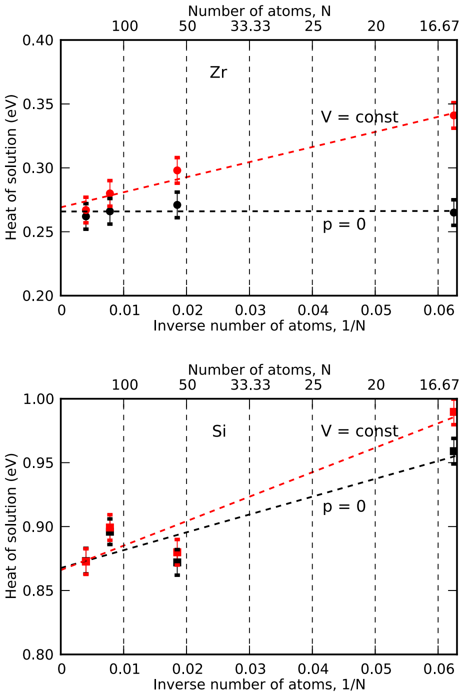

Fig. 1. Calculated heat of solution H_{s} of (a) Zr and (b) Si in molybdenum as a function of inverse number of atoms in the supercell $1/N$. Two types of boundary conditions are considered: $p \approx 0$ and $V = \mathrm{const}$. The energies relating to a infinite crystal are obtained by a linear extrapolation to $1/N \rightarrow 0$.

Table 2. Calculated heat of solution, formation volume and theoretical solubility limit of Zr and Si in molybdenum at the respective peritectic temperature.

	H_{s} (eV)	$\Delta V/\Omega$	c (at.%)	c^{exp} (at.%)
Zr	0.27 ± 0.03	0.16	23 ± 3	≈ 3–20 [7,9,10]
Si	0.87 ± 0.03	−0.1	1.1 ± 3	≈4 [13–15]